

## Discovery and SAR of oxindole–pyridine-based protein kinase B/Akt inhibitors for treating cancers

Gui-Dong Zhu,<sup>a,\*</sup> Viraj B. Gandhi,<sup>a</sup> Jianchun Gong,<sup>a</sup> Yan Luo,<sup>a</sup> Xuesong Liu,<sup>a</sup> Yan Shi,<sup>a</sup> Ran Guan,<sup>a</sup> Shayna R. Magnone,<sup>a</sup> Vered Klinghofer,<sup>a</sup> Eric F. Johnson,<sup>a</sup> Jennifer Bouska,<sup>a</sup> Alexander Shoemaker,<sup>a</sup> Anatol Oleksijew,<sup>a</sup> Ken Jarvis,<sup>a</sup> Chang Park,<sup>b</sup> Ron De Jong,<sup>c</sup> Tilman Oltersdorf,<sup>c</sup> Qun Li,<sup>a</sup> Saul H. Rosenberg<sup>a</sup> and Vincent L. Giranda<sup>a</sup>

<sup>a</sup>Cancer Research, GPRD, Abbott Laboratories, Abbott Park, IL 60064, USA

<sup>b</sup>Structural Biology, GPRD, Abbott Laboratories, Abbott Park, IL 60064, USA

<sup>c</sup>IDUN Pharmaceuticals Inc., 9380 Judicial Drive, San Diego, CA 92121, USA

Received 10 March 2006; revised 31 March 2006; accepted 3 April 2006

Available online 27 April 2006

**Abstract**—We describe a series of potent and selective oxindole–pyridine-based protein kinase B/Akt inhibitors. The most potent compound **11n** in this series demonstrated an IC<sub>50</sub> of 0.17 nM against Akt1 and more than 100-fold selectivity over other Akt isozymes. The selectivity against other protein kinases was highly dependent on the C-3 substitutions at the oxindole scaffold, with unsubstituted **9e** or 3-furan-2-ylmethylene (**11n**) more selective and 3-(1*H*-pyrrol-2-yl)methylene (**11f**) or 3-(1*H*-imidazol-2-yl)methylene (**11k**) less selective. In a mouse xenograft model, **9d**, **11f**, and **11n** inhibited tumor growth but with accompanying toxicity. © 2006 Elsevier Ltd. All rights reserved.

Protein kinases are a large family of diverse but related enzymes that regulate nearly all aspects of cell growth, differentiation, and division. Dys-regulation of one or more protein kinases has been associated with a wide spectrum of human cancers. Partially encouraged by the clinical success of Gleevec (inhibitor of BCR-ABL, PDGFR, and c-Kit), as well as Iressa (EGFR inhibitor), a search for small molecule inhibitors of protein kinases as anti-cancer chemotherapeutics has received increasing attention.<sup>1</sup> Among the superfamily of protein kinases, protein kinase B, also called Akt, is a pivotal component of the phosphatidylinositol 3'-kinase/Akt signal transduction pathway that regulates many processes crucial to carcinogenesis.<sup>2</sup> Overexpression of Akt as a result of, for example, inactivation of tumor suppressor PTEN has been found in a variety of human tumors.<sup>3</sup> At the genomic level, Akt1 and Akt2 have been shown to be amplified in many cancer types.<sup>4</sup> Therefore, Akt has long been considered an attractive target for the treatment of cancers. There have been a number of small

molecule inhibitors that partially target Akt.<sup>1</sup> While the majority of these inhibitors are ATP-competitive, Lindsay et al. reported a series of selective allosteric and non-ATP-competitive diphenylquinoxaline- and diphenylpyridine-based inhibitors of Akt that target the pleckstrin homology (PH) domain of the protein kinase.<sup>5,6</sup>

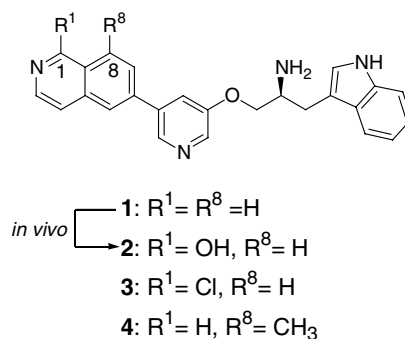


**Figure 1.** Compound **2** was assigned as a major metabolite of Akt inhibitor **1** in several species. Blocking the C-1 site of metabolism of the isoquinoline provided compounds, for example, **3** or **4**, with respectable pharmacokinetic profile but with diminished Akt activity.

**Keywords:** Akt inhibitor; Protein kinase B; PKB; GSK3; FL5.12-Akt; Anticancer.

\* Corresponding author. Tel.: +1 847 935 1305; fax: +1 847 935 5165; e-mail: gui-dong.zhu@abbott.com

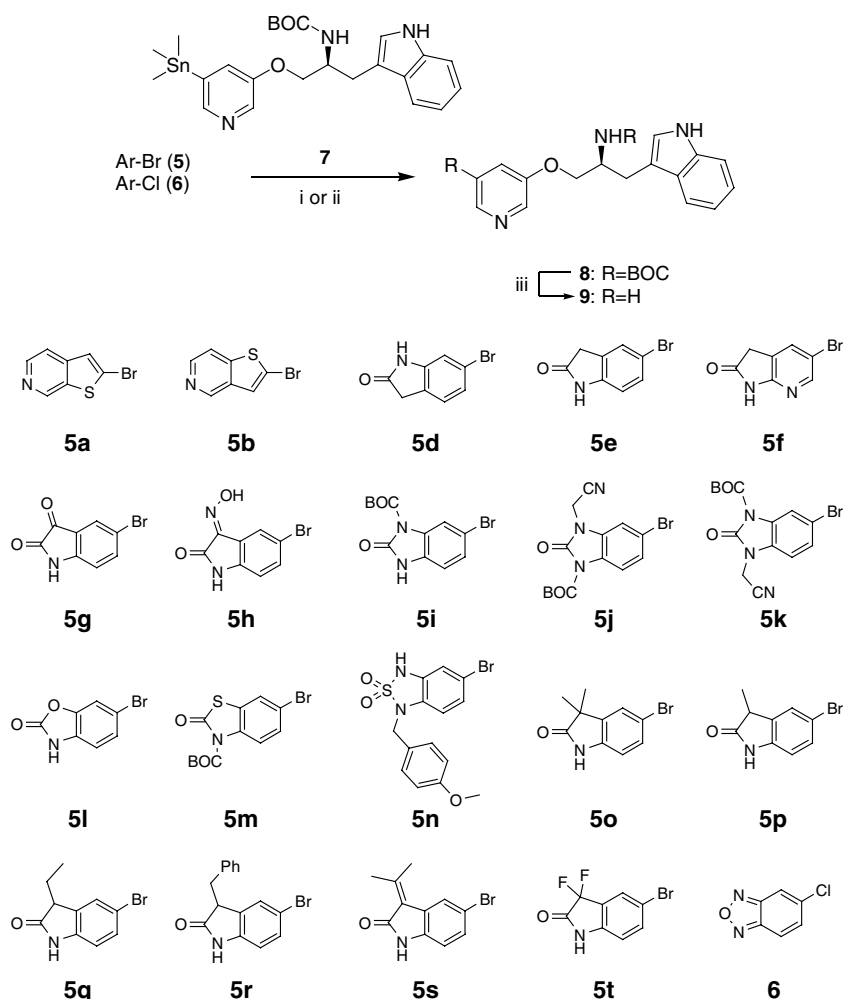
We previously described a novel, potent ( $IC_{50} = 2.0$  nM), and selective Akt inhibitor **1** and showed significant efficacy in several mouse xenograft models<sup>7</sup> (see Fig. 1). Major shortcomings of this Akt inhibitor as a clinically useful agent include short half-life in animals and poor oral bio-availability. The C-1 position of the isoquinoline was identified as a major site of metabolism, however, any modification failed to provide potency against Akt.<sup>8</sup> Herein, we have explored a number of alternative heterocyclic scaffolds to replace the metabolically labile isoquinoline, and describe a new series of potent and selective oxindole–pyridine based inhibitors.

Depicted in Scheme 1 is a general synthesis of compounds **9a–9t**. Stille reactions of either an arylbromide **5** or arylchloride **6** with trimethylstannane **7**,<sup>8</sup> under the catalysis of tri-*o*-tolylphosphine (for bromide **5**) or 2-dicyclo-hexylphosphino-2'-(*N,N*-dimethyl-amino)biphenyl(Cy-MAP, for chloride **6**), provided compound **8**. Treatment of **8** with trifluoroacetic acid in methylene chloride afforded Akt inhibitor **9**. **5d**, **5e**, **5g**, and **6** were all commercially available, while **5a**,<sup>9</sup> **5b**,<sup>9</sup> **5f**,<sup>10</sup> **5i**,<sup>11</sup> **5j**,<sup>11</sup> **5k**,<sup>11</sup> **5l**,<sup>12</sup> **5m**,<sup>12</sup> and **5n**<sup>13</sup> were prepared according to literature procedures. Aryl bromides **5o–5r** were obtained

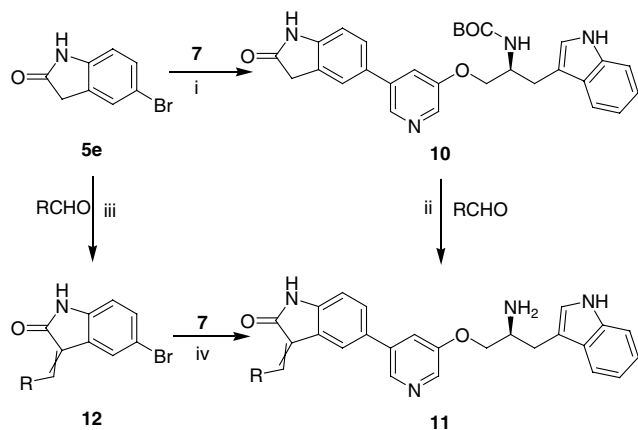
through alkylation of 5-bromoindole **5e** with the appropriate alkyl halides in the presence of base. Condensation of **5e** with acetone and **5g** with hydroxylamine provided aryl bromides **5s** and **5h**. Fluorination of the isatin **5g** with DAST under standard conditions ( $CH_2Cl_2$ , rt) afforded difluoro-analog **5t**.

The synthesis of Akt inhibitors **11a–11p** is outlined in Scheme 2. Stille coupling of 5-bromoindole **5e** with trimethylstannane **7** in the presence of  $Pd_2(dba)_3$  and (*o*-tol)<sub>3</sub>P furnished **10** in 47% yield. Treatment of **10** with a variety of aldehydes in the presence of piperidine afforded, after BOC-deprotection, compounds **11a–11p** in poor to modest yields. Alternatively, these compounds (except for **11h**) could be prepared on larger scale by initial condensation with an aldehyde, followed by Stille reaction in improved overall yield. The stereochemistry of the exo-indole double bond was deduced from related analogs in the literature<sup>14</sup> and confirmed by <sup>1</sup>H NMR NOE studies. The ratio of the geometric isomers was calculated from their <sup>1</sup>H NMR spectra.

Table 1 highlights the heterocyclic scaffolds that we investigated as potential replacements for the



**Scheme 1.** Reagents and conditions. For Ar-Br: (i)  $Pd_2(dba)_3$ ,  $P(o\text{-tol})_3$ ,  $Et_3N$ , DMF, 80 °C, 6 h. For Ar-Cl: (ii) 2-dicyclohexylphosphino-2'-(*N,N*-dimethylamino)biphenyl(Cy-MAP),  $Pd_2(dba)_3$ ,  $Et_3N$ , DMF, 80 °C, overnight; (iii)  $CF_3CO_2H$ .



**Scheme 2.** Reagents and conditions: (i) Pd<sub>2</sub>(dba)<sub>3</sub>, P(*o*-tol)<sub>3</sub>, Et<sub>3</sub>N, DMF, 80 °C, 6 h, 47%; (ii) a—piperidine, MeOH, 60 °C, overnight; b—CF<sub>3</sub>CO<sub>2</sub>OH, CH<sub>2</sub>Cl<sub>2</sub>; (iii) piperidine, MeOH, 60 °C, overnight; (iv) a—Pd<sub>2</sub>(dba)<sub>3</sub>, P(*o*-tol)<sub>3</sub>, Et<sub>3</sub>N, DMF, 80 °C, 6 h; b—CF<sub>3</sub>CO<sub>2</sub>OH, CH<sub>2</sub>Cl<sub>2</sub>.

isoquinoline pharmacophore in compound **1**. Replacement of the isoquinoline with the isosteric thieno[2,3-*c*]pyridine, known to have good pharmacokinetic properties, resulted in a compound (**9a**) with slightly reduced potency in the enzyme assay (IC<sub>50</sub> = 5.4 nM) and with comparable activity in a MTT assay (IC<sub>50</sub> = 0.39 μM vs 0.35 μM for **1**).<sup>15</sup> Thieno[3,2-*c*]pyridine isostere (**9b**), on the other hand, was much less active, with an IC<sub>50</sub> of 488 nM. Substitution with benzofurazan (**9c**), while the oxygen atom could mimic the hinge-binding nitrogen of the isoquinoline in **1**, led to more than an order of magnitude drop in potency against Akt1. Replacement of the isoquinoline nitrogen with a carbonyl group led to oxindole analogs **9d** and **9e**. While **9d** was essentially inactive, **9e** showed a respectable IC<sub>50</sub> of 3.1 nM against Akt1. We postulated that incorporation of a nitrogen atom into the phenyl ring or introduction of another carbonyl at 3-position of the oxindole would increase the basicity of the 2-oxo group, therefore making the 2-carbonyl a better hydrogen bond acceptor. Unfortunately, both modifications (**9f**, **9g**) led to a reduction in potency. An oxime analog (**9h**), however, showed a respectable IC<sub>50</sub> against Akt (IC<sub>50</sub> = 6.5 nM).

We also replaced the metabolically labile C-3 methylene of the oxindole scaffold of **9e** with nitrogen atom, forming a potentially more stable cyclic urea structure. Again, this modification resulted in compounds (**9i**, **9j**) with much diminished activity against Akt. An oxygen or sulfur substitution for this methylene, however, was found to provide compounds (**9l**, **9m**) with single digit nanomolar IC<sub>50</sub> against Akt1. A sulfanamide analog (**9n**) was nearly inactive (Akt1 IC<sub>50</sub> = 15.6 μM). Alkylation of the C-3 oxindole methylene with methyl, ethyl, or benzyl groups led to compounds **9o–9r**, with monomethyl analog **9p** the most potent (IC<sub>50</sub> = 4 nM). The geminal difluoro-analog **9t** was 2-fold more potent than compound **9e** against Akt1, but, unexpectedly, was much less cytotoxic in a MTT assay (IC<sub>50</sub> = 11.8 μM).

**Table 1.** Enzyme and cellular assay results for compounds **1** and **9a–9t**

Compound	R	Akt1 IC <sub>50</sub> <sup>a</sup> (nM)	MTT (F5.12-Akt) IC <sub>50</sub> <sup>a</sup> (μM)
<b>1</b>		2.0	0.42
<b>9a</b>		5.4	0.39
<b>9b</b>		488	nd <sup>b</sup>
<b>9c</b>		41	8.7
<b>9d</b>		4400	nd
<b>9e</b>		3.2	0.94
<b>9f</b>		99	40
<b>9g</b>		179	nd
<b>9h</b>		6.5	30
<b>9i</b>		147	40
<b>9j</b>		405	nd
<b>9k</b>		20,700	nd
<b>9l</b>		7.4	0.62
<b>9m</b>		4.3	1.3
<b>9n</b>		15,600	nd
<b>9o</b>		24.6	2.7

Table 1 (continued)

Compound	R	Akt1 IC <sub>50</sub> <sup>a</sup> (nM)	MTT (F5.12-Akt) IC <sub>50</sub> <sup>a</sup> (μM)
9p		4.0	1.5
9q		80	nd
9r		1020	nd
9s		52.7	1.88
9t		1.5	11.8

<sup>a</sup> Values are means of two or more experiments. All compounds were tested under 5 μM ATP.

<sup>b</sup> Not determined.

SAR studies of **9e** analogs with olefinic substitutions at the C-3 position of the oxindole are summarized in Table 2. In general, mono-substituted exomethylene analogs displayed better binding affinity to Akt than the bis-substituted analogs (e.g., **9s** in Table 1, IC<sub>50</sub> = 52.7 nM). Relatively smaller groups tended to give the best activity. The more sterically hindered dichlorophenyl analog **11c** resulted in a 50-fold drop in Akt activity. Incorporation of a nitrogen at the *meta*-(**11d**) or *ortho*-(**11e**) position of the phenyl ring was also detrimental.

Installation of a 2-pyrrole at the exo-methylene provided compound **11f** with a respectable IC<sub>50</sub> of 1.5 nM against Akt1. N-methylation on the pyrrole ring afforded compound **11h** with slightly reduced activity, while saturation of the ring led to a much less active **11g** (IC<sub>50</sub> = 660 nM). The 3-pyrrole analog **11i** was equally potent as its C-2 regioisomer. An indole analog **11j** was found to be two orders of magnitude less active than **11i**. Multiple alkyl substitutions on the pyrrol-2-yl group of **11f** were also detrimental (**11l**). 3*Z*-Imidazol-2-yl (**11k**) showed a 5-fold reduction in potency relative to 3*Z*-pyrrol-2-yl analog **11f**. Unexpectedly, a thiophene analog **11m** was 5-fold more potent than its isostere phenyl analog **11b**. As shown in Table 2, 2-furyl analog **11n** demonstrated superior potency over all other analogs investigated so far, with an IC<sub>50</sub> of 0.17 nM. Since the IC<sub>50</sub> was lower than the enzyme concentration (0.5 nM), the given number was determined by interpolation (curve-fitting). Reduction in activity was observed with mono- or multiple alkyl substitution of the furan ring (**11o** and **11p**).

Table 2. Geometry ratios of the exo-oxindole double bond, enzyme and cellular assay results for compounds **11a–11p**

Compound	R	Z/E ratio	Akt1 IC <sub>50</sub> <sup>a</sup> (nM)	MTT (F5.12-Akt) IC <sub>50</sub> <sup>a</sup> (μM)
11a		1:1	3.3	2.0
11b		1:1	5.9	2.2
11c		1:1	352	nd <sup>b</sup>
11d		1:3	10.4	4.8
11e		>98:1	10.3	1.3
11f		>98:1	1.5	0.2
11g		>98:1	660	nd
11h		2:3	8.2	1.20
11i		1:1	1.2	0.45
11j		1:9	153	nd
11k		>98:1	7.2	0.25
11l		>98:1	40.3	3.2
11m		3:1	0.9	0.83
11n		1:8	0.17	0.4
11o		1:9	0.7	0.4
11p		1:9	10	0.97

<sup>a</sup> Values are means of two or more experiments. All compounds were tested under 5 μM ATP.

<sup>b</sup> Not determined.

Because of potential protein-induced *cis/trans* isomerization of the ligand, it is hard to draw any conclusions from aforementioned SAR. They can be the substituting effects on the exo-double bond or just a reflection of a Z/E ratio of these substituents in the ligand/protein complexes. Several attempts to co-crystallize compounds in this series with purified Akt, Akt-mutated PKA and/or PKA protein failed to provide a single

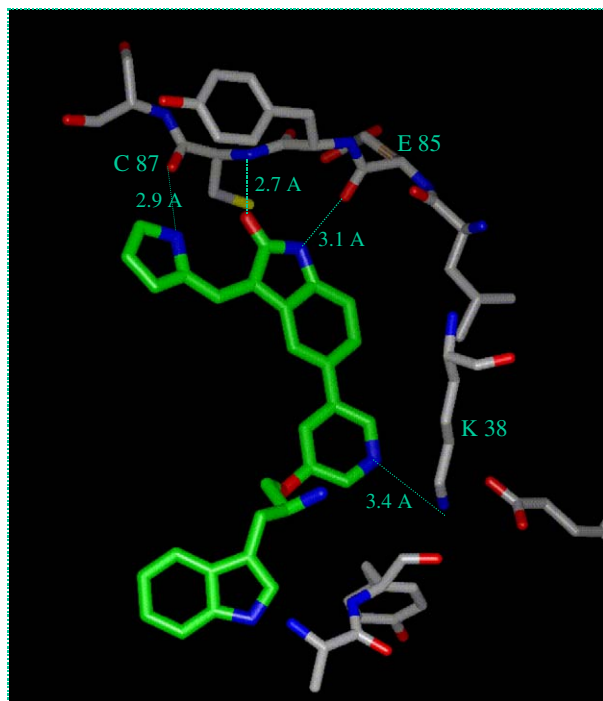


**Figure 2.** X-ray structure of **11f** in Chk-1 kinase. The pyrrol-2-yl group in **11f** orients in *cis*-configuration to the carbonyl of the oxindole scaffold in the ligand/protein complex.<sup>16</sup>

crystal with sufficient quality for X-ray study. However, an X-ray structure of **11f** in a less related Chk-1 kinase demonstrated an exclusive *cis*-configuration of the pyrrole to the carbonyl of the oxindole in the ligand/protein complex. The pyrrole nitrogen, the oxindole nitrogen, and carbonyl formed three hydrogen bonds with the backbone peptides in the hinge region (see Fig. 2).

To further evaluate this series of Akt inhibitors and understand the lack of correlation between the enzyme activity and cytotoxicity, several representative compounds were screened for kinase selectivity. As summarized in Table 3, oxindoles **9e** and **11n** demonstrated

**Table 3.** Fold-selectivity of Akt inhibitors for Akt1 over selected kinases<sup>a</sup>

Kinase	<b>1</b>	<b>9e</b>	<b>11f</b>	<b>11k</b>	<b>11n</b>
Akt1	1	1	1	1	1
Akt2	5	8	5	nd <sup>b</sup>	130
Akt3	27	110	43	19	100
PKA	1.6	110	2	1	280
PKC $\gamma$	210	570	40	2	1500
PKC $\xi$	9200	>16,000	12,000	5700	>50,000
CDK1	77	790	4	0.4	3700
ERK2	700	300	220	nd	1700
CK2	9100	>16,000	1900	56	>50,000
SRC	>1000	1200	15	17	440

<sup>a</sup> The fold-selectivity for Akt1 over selected protein kinases is shown for each selected Akt inhibitor. The listed kinases are those relatively less selective for other series of Akt inhibitors and belong to AGC (PKA, PKC), TK (SRC), and CMGC (CDK1, ERK2, CK2) family of protein kinases.

<sup>b</sup> Not determined.

good selectivity against most of the protein kinases we tested and were more selective than the isoquinoline-based benchmark inhibitor **1** versus, for example, PKA (110- and 280-fold vs 1.6-fold) and CDK1 (790- and 3700-fold vs 77-fold). On the other hand, the 2-pyrrole analog **11f** and 2-imidazole analog **11k** were less selective in general against most of the kinases we tested. The much wider spectrum of kinase activity of **11f** and **11k** is probably responsible for the higher cytotoxicity of both compounds (MTT IC<sub>50</sub> = 0.2  $\mu$ M for **11f** and 0.25  $\mu$ M for **11k**, Table 4).

One of the major goals in exploring an alternative pharmacophore for the isoquinoline in compound **1** was to improve the pharmacokinetic properties. However, a mouse PK screening of the oxindole series of Akt inhibitors revealed a similar profile as isoquinoline compound **1**. There was no oral drug plasma levels observed with these compounds in mice, with <10% oral bioavailability observed for compound **11f** in rat.

Due to the lack of oral bioavailability, compounds **9e**, **11f**, and **11n** were administered subcutaneously in separate MiaPaCa-2 mouse xenograft models at the maximum tolerable doses. As highlighted in Table 5, the most potent Akt inhibitor **11n** showed modest efficacy, while the less potent inhibitor **11f** demonstrated significantly better efficacy in slowing tumor growth. However, more toxicity, including lethargy, weight loss, and skin irritation at the site of injection, were repeatedly observed after administration of **11f**. Compound **9e** showed similar efficacy as **11n** in the MiaPaCa model at 5-fold higher doses (75 mg/kg). Both **9e** and **11n** also displayed a similar spectrum of toxicity as **11f** but to a significantly less extent.

In an effort to elucidate the superior efficacy of compound **11f** in the MiaPaCa models over **9e** and **11n**,

**Table 4.** Cellular activity of selected Akt inhibitors in comparison with **1** (IC<sub>50</sub>,  $\mu$ M)<sup>a</sup>

Cell	<b>1</b>	<b>9e</b>	<b>11f</b>	<b>11k</b>	<b>11n</b>
GSK3-P	1.5	1.94	0.9	5.0	2.5
FL5.12-Akt (MTT)	0.42	0.94	0.20	0.25	0.40
MiaPaCa-2 (MTT)	0.59	1.71	0.14	0.085	0.88

<sup>a</sup> Values are means of two or more experiments.

**Table 5.** Summary of the efficacies in MiaPaCa-2 mouse xenograft models<sup>17</sup> for selected Akt inhibitors in comparison to Gemzar<sup>a</sup>

Compound	Dose (mg/kg/day)	Route	Dose schedule	T/C at #day
<b>9e</b>	75	sc	Bid; d1–21	60% at d28
<b>11f</b>	25	sc	Bid; d1–7	13% at d15
<b>11n</b>	15	sc	Bid; d1–17	69% at d24
Gemzar	120	ip	Qd; d3, 6, 9, 12	34% at d21

<sup>a</sup> All Akt inhibitors were subcutaneously dosed twice daily as indicated schedules after inoculation. Tumor size was measured at specified days with digital calipers. The data were from different trials with a similar efficacy for Gemzar as control. All animals were humanely euthanized on indicated days due to development of toxicity.

phosphorylation of the Akt downstream target GSK3 was measured in the presence of inhibitor. The results are summarized in Table 4 together with their cytotoxicity in MiaPaCa-2 cells. The higher cellular activity of **11f** for GSK3 phosphorylation (0.9 vs 1.94  $\mu\text{M}$  and 2.5  $\mu\text{M}$  for **9e** and **11n**) and cell-killing in MiaPaCa correlated well with their in vivo efficacy.

In summary, we have developed a series of potent and selective oxindole-pyridine-based Akt inhibitors. The most potent compound **11n** had an  $\text{IC}_{50}$  of 0.17 nM against Akt1 and was over 100-fold selective against other Akt isozymes. Compounds **9e** and **11n** were among the most selective Akt inhibitors in this series versus the closely related protein kinase A. Compounds **11f** and **11k** inhibited a much broader spectrum of protein kinases and showed higher cytotoxicity. In mouse MiaPaCa xenograft models, compounds **9e**, **11n**, and **11f** showed marginal to modest efficacy in inhibiting tumor growth but were accompanied by toxicity. The broader spectrum of activity of **11f** versus other kinases is likely responsible for its higher cytotoxicity, as well as an improved in vivo efficacy.

#### Acknowledgments

We thank Drs. Thomas Penning and Milan Bruncko for proofreading this manuscript and valuable suggestions.

#### References and notes

1. For reviews, see: (a) Barnett, S.; Bilodeau, M.; Lindsley, C. *Curr. Topics Med. Chem.* **2005**, *5*, 109; (b) Li, Q.; Zhu, G.-D. *Curr. Topics Med. Chem.* **2002**, *2*, 939.
2. For a review, see: Nicholson, K. M.; Anderson, N. G. *Cell. Signal.* **2002**, *14*, 381.
3. For reviews, see: (a) Vivanco, I.; Sawyers, C. *Nat. Rev. Drugs* **2004**, *13*, 787.
4. Staal, S. *Proc. Natl. Acad. Sci. U.S.A.* **1987**, *84*, 5034.
5. (a) Lindsley, C.; Zhao, Z.; Leister, William, H.; Robinson, R.; Barnett, S.; Defeo-Jones, D.; Jones, R.; Hartman, G.; Huff, J.; Huber, H.; Duggan, M. *Bioorg. Med. Chem. Lett.* **2005**, *15*, 761; (b) Barnett, S.; Defeo-Jones, D.; Fu, S.; Hancock, P.; Haskell, K.; Jones, R.; Kahana, A.; Kral, A.; Leander, K.; Lee, L.; Malinowski, J.; McAvoy, E.; Nahas, D.; Robinson, R.; Huber, H. *Biochem. J.* **2005**, *385*(Pt. 2), 399.
6. Zhao, Z.; Leister, W.; Robinson, R.; Barnett, S.; Defeo-Jones, D.; Jones, R.; Hartman, G.; Huff, J.; Huber, H.; Duggan, M.; Lindsley, C. *Bioorg. Med. Chem. Lett.* **2005**, *15*, 905.
7. (a) Luo, Y.; Shomaker, A.; Liu, X.; Woods, K.; Thomas, S.; de Jong, R.; Han, E.; Li, T.; Stoll, V.; Powlas, J.; Oleksijew, A.; Mitten, M.; Shi, S.; Guan, R.; McGonigal, T.; Klinghofer, V.; Johnson, E.; Levenson, J.; Bouska, J.; Mamo, M.; Smith, R.; Gramling-Evans, E.; Zinker, B.; Mika, A.; Nguyen, P.; Oltersdorf, T.; Rosenberg, S.; Li, Q.; Giranda, V. *Mol. Cancer Ther.* **2005**, *4*, 977; (b) Li, Q.; Woods, K.; Thomas, S.; Zhu, G.-D.; Packard, G.; Fisher, J.; Li, T.; Gong, J.; Dinges, J.; Song, X.; Abrams, J.; Luo, Y.; Johnson, E.; Shi, S.; Liu, X.; Klinghofer, V.; de Jong, R.; Oltersdorf, T.; Stoll, V.; Jakob, C.; Rosenberg, S.; Giranda, V. *Bioorg. Med. Chem. Lett.* **2006**, *16*, 2000.
8. Zhu, G.-D.; Gong, J.; Claibone, A.; Woods, K.; Gandhi, V.; Thomas, S.; Luo, Y.; Liu, X.; Shi, S.; Guan, R.; Magnone, S.; Klinghofer, V.; Johnson, E.; Bouska, J.; Shoemaker, A.; Oleksijew, A.; Stoll, V.; de Jong, R.; Oltersdorf, T.; Li, Q.; Rosenberg, S.; Giranda, V. *Bioorg. Med. Chem. Lett.* **2006**, in press.
9. Wikel, J.; Denney, M.; Vasileff, R. *J. Heterocycl. Chem.* **1993**, *30*, 289.
10. Mazeas, D.; Guillaumet, G.; Viaud, M.-C. *Heterocycles* **1999**, *50*, 1065.
11. Takeda, K.; Ogura, H. *Synth. Commun.* **1982**, *12*, 213.
12. Makosza, M.; Sienkiewicz, K. *J. Org. Chem.* **1998**, *63*, 4199.
13. Carson, J. US Patent 3,177,221, 1965.
14. Sun, L.; Tran, N.; Tang, F.; App, H.; Hirth, P.; McMahon, G.; Tang, C. *J. Med. Chem.* **1998**, *41*, 2588.
15. Zhu, G.-D.; Arendsen, D.; Gunawardana, I.; Boyd, S.; Stewart, A.; Fry, D.; Cool, B.; Kifle, L.; Schaefer, V.; Meuth, J.; Marsh, K.; Kempf-Grote, A.; Kilgannon, P.; Gallatin, M.; Okasinski, G. *J. Med. Chem.* **2001**, *44*, 3469.
16. Compound **11f** was soaked into the native Chk-1 kinase crystals that were obtained in a solution containing 20 mg/mL of the protein and PKI peptide. The structure of the ligand/protein complex was determined and refined to a resolution of 3.5 Å ( $R_{\text{work}} = 22.1\%$  and  $R_{\text{free}} = 31.9\%$ ). Crystallographic data described in this paper have been deposited with PDB (ID: 2GHG).
17. Animal studies were conducted following the guidelines of the internal Institutional Animal Care and Use Committee. Immunocompromised male scid mice (C.B-17-Prkdc<sup>scid</sup>) were randomly assigned to treatment groups and therapy was initiated the day after inoculation. Ten animals were assigned to each group, including controls. MiaPaCa-2 cells were obtained from the American Type Culture Collection (Manassas, VA).  $2 \times 10^6$  MiaPaCa-2 cells in 50% Matrigel (BD Biosciences, Bedford, MA) were inoculated subcutaneously into the flank. Tumor size was evaluated by twice weekly measurements with digital calipers. Tumor volume was estimated using the formula:  $V = L \times W^2/2$ .